Structural transitions and elasticity from torque measurements on DNA

Zev Bryant*, Michael D. Stone*, Jeff Gore†, Steven B. Smith†‡, Nicholas R. Cozzarelli* & Carlos Bustamante*†‡§

** Department of Molecular and Cell Biology, † Department of Physics, ‡ Howard Hughes Medical Institute, and § Physical Biosciences Division of Lawrence Berkeley National Laboratory, University of California, Berkeley, California 94720, USA*

Knowledge of the elastic properties of DNA is required to understand the structural dynamics of cellular processes such as replication and transcription. Measurements of force and extension on single molecules of DNA[1–3] have allowed direct determination of the molecule's mechanical properties, provided rigorous tests of theories of polymer elasticity[4], revealed unforeseen structural transitions induced by mechanical stresses[3,5–7], and established an experimental and conceptual framework for mechanical assays of enzymes that act on DNA[8]. However, a complete description of DNA mechanics must also consider the effects of torque, a quantity that has hitherto not been directly measured in micromanipulation experiments. We have measured torque as a function of twist for stretched DNA—torsional strain in over- or underwound molecules was used to power the rotation of submicrometre beads serving as calibrated loads. Here we report tests of the linearity of DNA's twist elasticity, direct measurements of the torsional modulus (finding a value ~40% higher than generally accepted), characterization of torque-induced structural transitions, and the establishment of a framework for future assays of torque and twist generation by DNA-dependent enzymes. We also show that cooperative structural transitions in DNA can be exploited to construct constant-torque wind-up motors and force–torque converters.

Previous investigations of the force–extension behaviour of supercoiled DNA have found that, under low tension, DNA behaves like an isotropic flexible rod[2,9]: as turns are added to the molecule, its extension remains nearly constant until a critical twist density is reached and the molecule buckles to form plectonemic (interwound) structures; thereafter, additional turns cause a rapid decrease in extension as twist is traded for writhe. At higher tensions, the behaviour of over- and underwound molecules differ. In each case, DNA undergoes a structural change before the twist density necessary for buckling is reached, and the molecule lengthens (or contracts only gradually) as additional turns are introduced[6,7]. These results have been interpreted to reflect cooperative torque-induced transitions in DNA structure[6,7], and a theoretical force–torque phase diagram has been proposed that explains the major features of force–extension curves for torsionally constrained molecules over a large range of forces and supercoiling densities[10]. Our work makes direct tests of both the isotropic rod model and the proposed force–torque phase diagram.

To perform dynamic torque measurements on single DNA molecules, we generated molecular constructs shown diagrammatically in Fig. 1a. The use of three distinct chemical modifications of DNA allows oriented tethering of the ends of the molecule, and attachment of a small bead (the 'rotor') to an internal position. A site-specific nick engineered below the rotor attachment point serves as a swivel.

We begin each assay by assembling the DNA molecule and rotor between two antibody-coated beads held in a micropipette and a force-measuring optical trap[11] (Fig. 1b and Supplementary Movie 1). Typically, we build up torsional stress in the molecule by holding the rotor bead stationary using fluid flow, and rotating the micropipette by ≥300 turns. When the flow is released, torque stored in the upper DNA segment causes the central bead to rotate continuously about its edge (Fig. 1c–e, and Supplementary Movies 2 and 3) until the torsional stress has been relieved, after which the bead rotates slightly back and forth under the influence of thermal fluctuations. Constant tension is maintained using force feedback[11], preventing buckling of the molecule[2] during the experiment, so that the observed dynamics reflect changes in twist and not writhe. At low Reynolds numbers, the magnitude of the torque can be determined as the product of the angular velocity (ω) of the rotor and its rotational drag (γ).

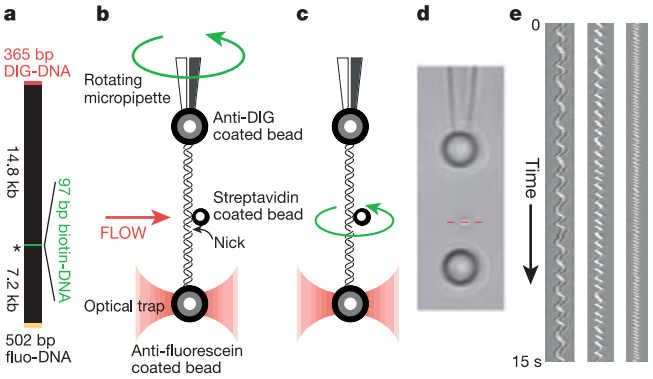

Figure 1 Experimental design. **a**, The molecular construct contains three distinct attachment sites and a site-specific nick (asterisk), which acts as a swivel. **b**, Each molecule was stretched between two antibody-coated beads using a dual-beam optical trap[11]. A rotor bead was then attached to the central biotinylated patch (see Supplementary Movie 1). The rotor was held fixed by applying a fluid flow, and the micropipette was twisted to build up torsional strain in the upper segment of the molecule. **c**, Upon releasing the flow, the central bead rotated to relieve the torsional strain. **d**, Video of the rotating bead (Supplementary Movies 2 and 3) was analysed to track cumulative changes in angle. Horizontal sections (red dashed line) of successive video frames can be stacked (**e**) to allow visualization of the helical path of the bead in space and time. Left to right, traces of 920 nm, 760 nm and 520 nm rotor beads.

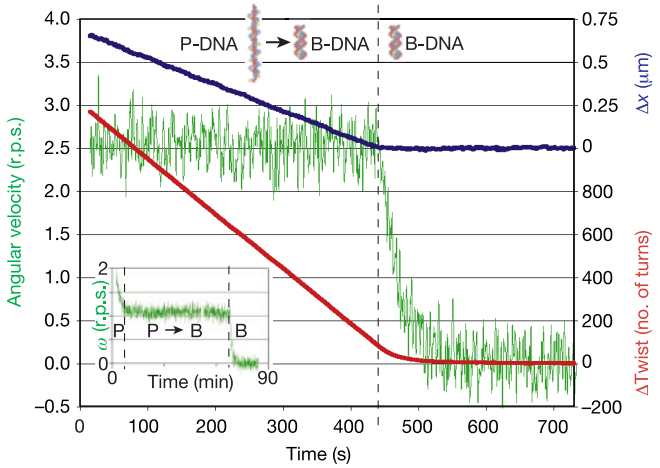

Figure 2 Analysis of bead rotation. A tether was overwound by 1,200 turns before releasing the 760 nm rotor bead. Red, cumulative rotor angle (Δtwist); green, angular velocity; and blue, molecular extension (Δx) versus time under constant tension (45 pN). The data support a model in which overwinding the molecule converts a fraction of the DNA into P-form[6,7]. P-DNA converts back into B-DNA at constant torque, after which the molecule regains its B-form extension and the remaining torque decays to zero. Inset, a molecule was completely converted to P-DNA by introducing 4,800 turns before releasing the 920 nm rotor bead. Torsional relaxation of hyperwound P-DNA preceded the long (~4,000 turns) P–B transition. During the gap at ~50 min, rotation was paused by turning on flow.

© 2003 Nature Publishing Group

In highly overwound DNA held at tensions >7 pN, a portion of the molecule is converted from standard B-DNA into an overextended, high-helicity form called P-DNA[6,7]. If the B → P transition is highly cooperative, it should occur at a constant torque. Confirming this prediction, the angular velocity of the rotor remained constant for much of the torsional relaxation of overwound molecules (Fig. 2). P to B conversion was reflected in a progressive reduction in extension. When all of the molecule had been converted to B-DNA, the extension ceased to change and the angular velocity of the rotor decayed to zero as the remaining torsional strain in the B-DNA was removed. Complete conversion of the 14.8 kilobase (kb) molecule into P-DNA (Fig. 2, inset) required the introduction of $\sim 4.0 \times 10^3$ turns, implying a helical repeat of ~2.7 base pairs (bp) per turn for P-DNA, close to previous estimates[6,7] of ~2.6 bp per turn. From the changes in extension at 45 pN, we conclude that P-DNA is 50% longer than B-DNA under our conditions (slightly shorter than previous estimates[6,7] of 60–75% longer than B-form).

To quantify the torques (τ) in our experiments, the angular velocity of the rotor during the P → B transition ($\omega_{P\rightarrow B}$) was measured using rotor beads of several different radii (r) (Fig. 3a, inset). The intended rotor geometry (a sphere rotating about its edge) was confirmed by video analysis, which showed that the orbital radius was equal to the bead radius (within a 2% error). This geometry predicts $\tau = \gamma\omega = 14\pi r^3 \eta\omega$, where η is the viscosity of the solution. The appearance of the expected relationship $\omega \propto r^{-3}$ allowed us to determine the critical torque of the P → B transition, $\tau_{crit,+} = 34 \pm 2$ pN nm (at 45 pN tension). This value was thereafter used as a calibration factor: instantaneous angular velocities of individual rotor beads were converted into torques using $\tau = \tau_{crit,+}(\omega/\omega_{P\rightarrow B})$.

To precisely determine the twist elasticity of DNA, numerous molecules were repeatedly over- or underwound and allowed to relax. Plots of torque as a function of twist show considerable run-to-run variation due to random thermal fluctuations (Fig. 3a). Therefore, torque–twist data from 103 runs were averaged together (Fig. 3b). The torque–twist relationship for DNA shows two constant-torque regions, reflecting structural transitions at $\tau_{crit,+} = +34$ pN nm and $\tau_{crit,-} = -9.6$ pN nm, and a nearly linear region reflecting the twist elasticity of B-DNA. Our direct measurements of $\tau_{crit,+}$ and $\tau_{crit,-}$ are in good agreement with previous estimates from force–extension analysis[6,7,9,12]. Entry into the 34 pN nm plateau can now be seen to be very sharp, demonstrating the cooperativity of the B–P transition. (Using Ising/Zimm-Bragg theory, we find that a free-energy penalty of at least $4k_BT$ at P–B domain boundaries is required to explain the data.) The transition at −9.6 pN nm is somewhat less cooperative (showing a shallow slope in the initial portion of the plateau), and probably reflects the formation of denatured DNA[6] and some combination of non-canonical structures (for example, Z-DNA[7,10]). Because the DNA has a net left-handed twist (~13 bp per turn; data not shown) upon completion of this transition[7,8,10], we have collectively designated the underwound states 'L-DNA'[8].

The twist elasticity of B-DNA is often assumed to be that of an isotropic rod: torque builds up linearly with twist according to $\tau = (C/L)(\theta - \theta_0)$, where L is the rod length, θ is the twisting angle, θ_0 is the equilibrium twist (35° per bp), and the torsional modulus C is constant. However, the asymmetry of twisting a chiral molecule suggests that this approximation may break down. Indeed, a study of fluorescence polarization anisotropy decay (FPA) reported a linear dependence of C on supercoiling density[13]. The anharmonic model proposed from FPA[13] fits our data better than a simple harmonic model (Fig. 3b). However, the deviation from linearity is small, accounting for a <10% reduction in torque near entry into the P–B transition.

The torsional modulus C of DNA (near $\theta - \theta_0 = 0$) has been

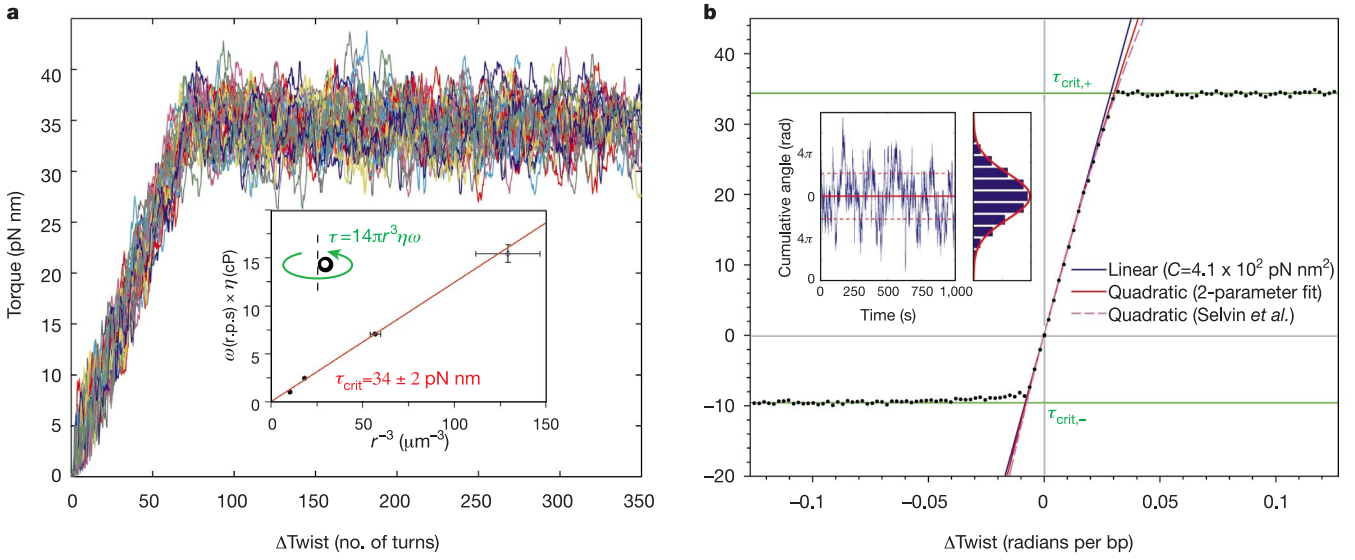

Figure 3 Torque calibration and twist elasticity of DNA. **a**, Torque versus twist for 37 runs from 16 molecules (520 nm rotor beads; 45 pN constant tension). Inset, calibration of $\tau_{crit,+}$. Angular velocities (ω) of beads with mean diameters of 920 nm ($n = 5$), 760 nm (n = 6) or 520 nm ($n = 16$) were measured during the P → B transition at 45 pN (filled circles, ±s.d.). Viscosity-corrected ω is proportional to r^{-3}; the best-fit slope (red) gives $\tau_{crit,+} = 34 \pm 2$ pN nm. Open circle, extrapolated P → B angular velocity for 400 nm beads ($n = 3$; see Methods). **b**, Averaged twist elasticity data. Negative torques: average of 39 runs at 15 pN. Positive torques: 37 runs at 45 pN and 27 runs at 15 pN gave very similar traces and were averaged together. Green lines, constant-torque structural transitions. Blue, linear fit to the data points falling within ±8 pN nm. Anharmonic models ($C(\Delta\theta) = a - b\Delta\theta/N$, where $N = 14{,}795$ bp) give superior fits to the data over the full range of B-DNA stability. Red, two-parameter anharmonic fit ($b/a = 4.5$); dashed purple, anharmonic fit constraining $b/a = 8.16$ to agree with FPA data[13]. Blue and red fits give $C(0) = 4.1 \times 10^2$ pN nm^2; purple fit gives $C(0) = 4.3 \times 10^2$ pN nm^2. Fits to 45 pN or 15 pN positive torque data alone (not shown) give $C(0) = 4.1 \times 10^2$ or 4.3×10^2 pN nm^2, respectively. Inset, independent measure of $C(0)$ using the equipartition theorem $\langle \Delta\theta^2 \rangle = k_BTL/C$, where $L = 5.03$ μm. Twist fluctuations of five molecules (520 nm rotor beads, 15 pN tension) were tracked at 50 Hz (example shown). Angular variance (red gaussian plot over blue data histogram) gives $C(0) = (4.4 \pm 0.4) \times 10^2$ pN nm^2.

© 2003 Nature Publishing Group

estimated from FPA[14,15], equilibrium topoisomer distribution of ligated circles[16,17], and circularization kinetics[18]. These methods give a wide range of values for C. FPA typically gives $C \approx 200\,\mathrm{pN\,nm^2}$, although elevated values have been reported for small circular DNA[15]. Topoisomer distribution analysis yields $C = 300$–$400\,\mathrm{pN\,nm^2}$, and best fits as high as $480\,\mathrm{pN\,nm^2}$ have been reported from circularization kinetics[18]. Theoretical treatments of force and extension data from single supercoiled DNA molecules[9,12,19,20] have yielded $C = 300\,\mathrm{pN\,nm^2}$ (ref. 19), $350\,\mathrm{pN\,nm^2}$ (refs 9, 12) and $C = 450\,\mathrm{pN\,nm^2}$ (ref. 20), depending on the analytical method. For all of the methods above, analytical theories or simulations are needed to estimate the relative contributions of twisting and bending or writhing to the experimental results. Topoisomer distributions of small circles (yielding $C \approx 300\,\mathrm{pN\,nm^2}$) have generally been considered the most reliable measurements, since the writhing contribution is thought to be small.

Our measurements provide a direct determination of C in the absence of writhe. A simple linear fit to the torque–twist data near $\theta - \theta_0 = 0$ gives $C = 410 \pm 30\,\mathrm{pN\,nm^2}$ (Fig. 3b). The uncertainty in this value depends heavily on imprecision in the absolute torque calibration from viscous drag (Fig. 2a, inset), since the relative scatter in the averaged data is small. To provide a drag-independent measure of C and check the calibration of our data, we used our experimental system to observe the amplitude of thermal fluctuations in twist (around $\theta - \theta_0 = 0$) and applied the equipartition theorem, as was previously done for single actin filaments[21]. This analysis (Fig. 3b, inset) yields $C = 440 \pm 40\,\mathrm{pN\,nm^2}$, in good agreement with our dynamic torque measurements.

These direct measurements of the torsional modulus of stretched DNA agree with the largest estimates of C from other methods, and are 40–50% higher than the widely used value of $\sim 300\,\mathrm{pN\,nm^2}$. The difference may be due to the presence of tension in our experiments. Stretching may induce structural changes that raise the torsional modulus, analogous to the proposed role of bending strain[15], or it may raise the effective C value owing to elastic coupling between twisting, bending and stretching (A. Matsumoto and W. Olson, personal communication). No increase in rigidity was observed between 15 pN and 45 pN, so any such effect must be saturated at these forces.

It is also possible that previous studies have not sufficiently accounted for writhing, and consequently underestimated the torsional rigidity. In this case, the only important role of tension is suppression of writhe fluctuations, which would otherwise lead to torsional softening[20]. Our measurement should then accurately reflect the local torsional modulus of the molecule.

We extended our analysis of torque and twist to investigate the overstretching transition of DNA (Fig. 4a). When DNA is pulled to high forces, it undergoes a cooperative transition at ~65 pN to a form ('S-DNA') that is 70% longer than B-form[3,5]. The structure of S-DNA remains the subject of debate[22], but it is known to be substantially underwound relative to B-DNA[7,10]. Therefore, untwisting must accompany overstretching. When our molecule-rotor assemblies are held at tensions above 65 pN, torque is generated that spins the rotor as the B → S transition progresses (Fig. 4a and Supplementary Movie 4). The ratio of changes in extension and twist ($\Delta x/\Delta\theta = 3.7$ nm per turn) corresponds to a helical repeat of ~33 bp per turn for S-DNA, slightly smaller than the previously reported value of 37.5 bp per turn[7,10]. Relaxation of the molecule below 65 pN allows complete rewinding to B-form twist. Higher tensions produce higher unwinding torques, following a Clausius–Clapeyron-like force–torque coexistence line for the B–S transition. Together with tension-dependent critical torque data for the P–B and L–B transitions, these measurements validate the proposed force–torque phase diagram for stretched and twisted DNA[10] (Fig. 4b).

We have shown that an over- or underwound DNA molecule behaves as a constant-torque wind-up motor capable of repeatedly producing thousands of rotations, and that an overstretched molecule acts as a force–torque converter. (During overstretching at forces above $F_{crit} \approx 65$ pN, the efficiency, ε, of converting force–extension work into rotational work is given by the Carnot-like expression $\varepsilon = 1 - F_{crit}/F$.) The production of continuous directed rotation by molecular devices has potential applications in the construction of nanomechanical systems. Previous approaches to this problem have included co-opting the biological motor F1 ATP synthase[23], which produces torques comparable to the P–B transition[23,24]. DNA-based devices that produce continuous rotation, according to the principles demonstrated here, might be integrated with existing DNA nanotechnology[25] using the intrinsic self-assembly properties of DNA.

An important future application of the methods developed here is the measurement of torque generation and changes in twist induced by DNA-associated enzymes. A previous measurement of torque generation by RNA polymerase[26] was complicated by buckling of the DNA to form plectonemes. Here, we have established a method for torque measurement that decouples twisting from writhing, with the potential for broad application to biological motors. □

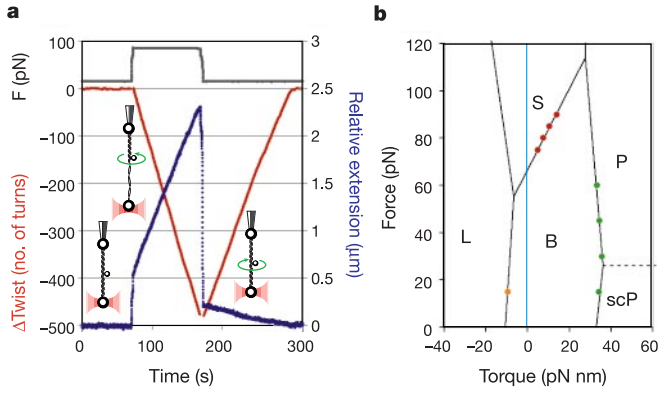

Figure 4 Unwinding during overstretching, and the global force–torque phase diagram of DNA. **a**, Unwinding during overstretching. Constructs were pulled to forces (black trace) above 65 pN. Cumulative rotations (red) of a 400 nm rotor bead showed continuous constant-torque untwisting while tension was maintained at 85 pN (Supplementary Movie 4). Concurrent decrease in twist (red) and increase in extension (blue) reflect S-DNA formation. When the force was relaxed to 15 pN, the molecule rewound, returning to B-form twist and extension. **b**, The global force–torque phase diagram of DNA. A single molecule was unwound by pulling to successively higher forces (relaxing at 15 pN between each run) to measure the torque of the B–S transition (judged from $\omega_{B \rightarrow S}$) as a function of force (red). The critical torque of the P–B transition was also measured as a function of force by relaxation of overwound tethers under varying tensions (green), and all critical torque data (orange: $\tau_{crit,-} = 9.6$ pN nm) were found to agree with a simple model[10] in which DNA can access five distinct structural states differing only in extension, twist, and free energy. scP, P-DNA that has been shortened by supercoiling[6,7].

Methods

Beads and molecular constructs

Beads (2.8 μm) coated with Protein G (Spherotech) were crosslinked to rabbit anti-fluorescein (Molecular Probes) or sheep anti-digoxigenin (DIG) (Roche). Streptavidin-coated rotor beads were purchased from Spherotech (760 nm) or Bangs (all others), and their diameters were measured from transmission electron micrographs using diffraction grating replicas as standards (400 nm, $n = 55$; 520 nm, $n = 81$; 760 nm, $n = 48$; 920 nm, $n = 66$); all beads appeared round.

Molecular constructs were generated by serial ligation of purified restriction fragments of chemically modified and unmodified DNA. Hapten-modified polymerase chain reaction (PCR) fragments (966 bp) were generated by amplification of a multiple cloning site using 0.2 mM dATP, dCTP and dGTP, 0.13 mM dTTP, and 0.07 mM biotin-dUTP, DIG-dUTP or fluorescein-dUTP (Roche). PCR fragments were digested and gel-purified to recover a 374 bp biotin-modified *Kpn*I fragment, a 365 bp DIG-modified *Bam*HI fragment, and a 502 bp fluorescein-modified *Cla*I fragment. pSV8 (a plasmid generated by

© 2003 Nature Publishing Group

insertion of the 5.5 kb *Bam*HI fragment of λ phage into pSV01[27]) was linearized with *Kpn*I, treated with alkaline phosphatase (AP), and ligated to an excess of the biotinylated *Kpn*I fragment. The product (containing nicked ligation junctions owing to the absence of plasmid-contributed phosphates) was digested with *Cla*I and *Xho*I. The resulting purified 7.3 kb fragment, designated protoSM, has the structure *Cla*I:7.2 kb:nick:97 bp(biotin-modified):*Xho*I. The torque-bearing DNA segment is the 14.8 kb *Bam*HI:*Sal*I fragment of pPIA6[28]. The final construct (SM1) was generated in a four-way ligation of the fluorescein-modified fragment, protoSM, torque-bearing segment, and DIG-modified fragment. Full-length products were selected by sequential binding to anti-fluorescein- and anti-DIG-coated beads in the optical tweezers. SM1 (Fig. 1a) was used in all reported experiments, with the following exceptions: SM2 (identical except DIG-DNA section extended to 601 bp for added stability) was used for the run shown in Fig. 2. SM3 (torque-bearing segment replaced with the 8.4 kb *Bgl*II-*Sal*I fragment of pSV8; fluorescein-DNA section extended to 4 kb) was used for the force–torque analysis of the B–S transition (red data points in Fig. 4b).

Experimental assembly and data collection

Anti-fluorescein beads were incubated with DNA and introduced into the flow chamber. Anti-DIG beads were introduced via a separate channel, and a molecular tether was assembled by keeping an anti-DIG bead on the micropipette by suction, and 'fishing' near a DNA:anti-fluorescein bead held in the laser trap. The trapped bead was then released into flow, and a streptavidin-coated 'rotor' bead was trapped and brought to the vicinity of the biotinylated portion of the molecule, where it became attached laterally to the DNA (Supplementary Movie 1). The micropipette was rotated using a computer-controlled electric motor (LEGO Mindstorms) while the rotor bead was held fixed by flowing buffer at $\sim$0.5 mm s^{-1}.

All experiments were performed in 100 mM NaCl and 40 mM Tris-HCl (pH 8.2). EDTA was typically present at 1 mM; omission caused no perceptible changes. Ambient temperature (23 $\pm$ 1 °C) was recorded prior to each experiment for use in viscosity calculations. Drag was also corrected for hydrodynamic coupling with the outer beads[29]; correction factors for the different rotor diameters were 1.005 (400 nm), 1.01 (520 nm), 1.02 (760 nm) and 1.03 (920 nm). Video was digitized at 30 Hz unless otherwise indicated, and the instantaneous angle of the rotor was extracted from the x-position and brightness (indicative of focal depth) of the bead. Angular velocities were obtained by numerical differentiation of the cumulative bead angle over a 1 s (Fig. 3) or 2 s (Fig. 2) window. The extrapolated P $\rightarrow$ B velocity of 400 nm beads (open circle in Fig. 3a inset) was obtained by measuring the velocity at large negative twists and scaling by $\tau_{\mathrm{crit},+}/\tau_{\mathrm{crit},-}$, since P $\rightarrow$ B rotation was too fast to track. During data collection, constant tension was maintained using stage-based force feedback[11]. During the exceptionally long run shown in Fig. 2 inset, force feedback (45 pN) was inoperative (out of actuator range) prior to $t = 23$ min, but $F > 30$ pN throughout.

Phase diagram

In the 'zero-temperature' approximation, the five-state structural model[10] leads to force–torque coexistence lines with constant slopes $\delta F/\delta\tau = -\Delta\theta/\Delta x$, where $\Delta\theta$ and Δx are the changes in twist and extension, respectively, for a particular structural transition. The slopes of the boundaries shown (Fig. 4b) were taken from experimental measurements of $\Delta\theta/\Delta x$, and predict the trends of the force–torque measurements. The intercepts of the boundaries were varied to fit the data. No torque measurements were made at the S–L or S–P boundaries, so these predicted slopes remain to be confirmed.

Received 6 February; accepted 28 May 2003; doi:10.1038/nature01810.

1. Smith, S. B., Finzi, L. & Bustamante, C. Direct mechanical measurements of the elasticity of single DNA molecules by using magnetic beads. *Science* **258,** 1122–1126 (1992).
2. Strick, T. R., Allemand, J. F., Bensimon, D., Bensimon, A. & Croquette, V. The elasticity of a single supercoiled DNA molecule. *Science* **271,** 1835–1837 (1996).
3. Smith, S. B., Cui, Y. & Bustamante, C. Overstretching B-DNA: The elastic response of individual double-stranded and single-stranded DNA molecules. *Science* **271,** 795–799 (1996).
4. Bustamante, C., Marko, J. F., Siggia, E. D. & Smith, S. Entropic elasticity of lambda-phage DNA. *Science* **265,** 1599–1600 (1994).
5. Cluzel, P. *et al.* DNA: An extensible molecule. *Science* **271,** 792–794 (1996).
6. Allemand, J. F., Bensimon, D., Lavery, R. & Croquette, V. Stretched and overwound DNA forms a Pauling-like structure with exposed bases. *Proc. Natl Acad. Sci. USA* **95,** 14152–14157 (1998).
7. Leger, J. F. *et al.* Structural transitions of a twisted and stretched DNA molecule. *Phys. Rev. Lett.* **83,** 1066–1069 (1999).
8. Bustamante, C., Bryant, Z. & Smith, S. B. Ten years of tension: Single-molecule DNA mechanics. *Nature* **421,** 423–427 (2003).
9. Bouchiat, C. & Mezard, M. Elasticity model of a supercoiled DNA molecule. *Phys. Rev. Lett.* **80,** 1556–1559 (1998).
10. Sarkar, A., Leger, J. F., Chatenay, D. & Marko, J. F. Structural transitions in DNA driven by external force and torque. *Phys. Rev. E* **63,** 051903 (2001).
11. Smith, S. B., Cui, Y. & Bustamante, C. Optical-trap force transducer that operates by direct measurement of light momentum. *Methods Enzymol.* **361,** 134–162 (2003).
12. Strick, T. R., Bensimon, D. & Croquette, V. Micro-mechanical measurement of the torsional modulus of DNA. *Genetica* **106,** 57–62 (1999).
13. Selvin, P. R. *et al.* Torsional rigidity of positively and negatively supercoiled DNA. *Science* **255,** 82–85 (1992).
14. Millar, D. P., Robbins, R. J. & Zewail, A. H. Direct observation of the torsional dynamics of DNA and RNA by picosecond spectroscopy. *Proc. Natl Acad. Sci. USA* **77,** 5593–5597 (1980).
15. Heath, P. J., Clendenning, J. B., Fujimoto, B. S. & Schurr, J. M. Effect of bending strain on the torsion elastic constant of DNA. *J. Mol. Biol.* **260,** 718–730 (1996).
16. Horowitz, D. S. & Wang, J. C. Torsional rigidity of DNA and length dependence of the free energy of DNA supercoiling. *J. Mol. Biol.* **173,** 75–91 (1984).
17. Shore, D. & Baldwin, R. L. Energetics of DNA twisting. II. Topoisomer analysis. *J. Mol. Biol.* **170,** 983–1007 (1983).
18. Crothers, D. M., Drak, J., Kahn, J. D. & Levene, S. D. DNA bending, flexibility, and helical repeat by cyclization kinetics. *Methods Enzymol.* **212,** 3–29 (1992).
19. Vologodskii, A. V. & Marko, J. F. Extension of torsionally stressed DNA by external force. *Biophys. J.* **73,** 123–132 (1997).
20. Moroz, J. D. & Nelson, P. Entropic elasticity of twist-storing polymers. *Macromolecules* **31,** 6333–6347 (1998).
21. Yasuda, R., Miyata, H. & Kinosita, K. Jr Direct measurement of the torsional rigidity of single actin filaments. *J. Mol. Biol.* **263,** 227–236 (1996).
22. Williams, M. C., Rouzina, I. & Bloomfield, V. A. Thermodynamics of DNA interactions from single molecule stretching experiments. *Acc. Chem. Res.* **35,** 159–166 (2002).
23. Soong, R. K. *et al.* Powering an inorganic nanodevice with a biomolecular motor. *Science* **290,** 1555–1558 (2000).
24. Yasuda, R., Noji, H., Kinosita, K. Jr & Yoshida, M. F1-ATPase is a highly efficient molecular motor that rotates with discrete 120 degree steps. *Cell* **93,** 1117–1124 (1998).
25. Seeman, N. C. DNA in a material world. *Nature* **421,** 427–431 (2003).
26. Harada, Y. *et al.* Direct observation of DNA rotation during transcription by *Escherichia coli* RNA polymerase. *Nature* **409,** 113–115 (2001).
27. Wobbe, C. R., Dean, F., Weissbach, L. & Hurwitz, J. *In vitro* replication of duplex circular DNA containing the simian virus 40 DNA origin site. *Proc. Natl Acad. Sci. USA* **82,** 5710–5714 (1985).
28. Davenport, R. J., Wuite, G. J., Landick, R. & Bustamante, C. Single-molecule study of transcriptional pausing and arrest by *E. coli* RNA polymerase. *Science* **287,** 2497–2500 (2000).
29. Davis, M. H. The slow translation and rotation of two unequal spheres in a viscous fluid. *Chem. Eng. Sci.* **24,** 1769–1776 (1969).

Supplementary Information accompanies the paper on **www.nature.com/nature**.

Acknowledgements We thank E. Watson and Y. Inclán for technical assistance, E. Nogales for microscope time, and A. Vologodskii, V. Croquette, D. Bensimon, D. Collin, N. Pokala and Y. Chemla for critical readings of the manuscript and/or discussions. Z.B. is an HHMI predoctoral fellow, M.D.S. is supported by a PMMB training grant, and J.G. holds a fellowship from the Hertz Foundation. This work was supported by the NIH and DOE.

Competing interests statement The authors declare that they have no competing financial interests.

Correspondence and requests for materials should be addressed to C.B. (carlos@alice.berkeley.edu).

Visualization of an unstable coiled coil from the scallop myosin rod

Yu Li*†‡, Jerry H. Brown*, Ludmilla Reshetnikova*, Antal Blazsek§, László Farkas§, László Nyitray§ & Carolyn Cohen*

** Rosenstiel Basic Medical Sciences Research Center, and † Biophysics and Structural Biology Program, Brandeis University, Waltham, Massachusetts 02454-9110, USA*
§ Department of Biochemistry, Eötvös Loránd University, Pázmány P. s. 1/c, 1117 Budapest, Hungary

α-Helical coiled coils in muscle exemplify simplicity and economy of protein design: small variations in sequence lead to remarkable diversity in cellular functions[1,2]. Myosin II is the key protein in muscle contraction, and the molecule's two-chain α-helical coiled-coil rod region—towards the carboxy terminus of the heavy chain—has unusual structural and dynamic features. The amino-terminal subfragment-2 (S2) domains of the rods can swing out from the thick filament backbone at a hinge in the coiled coil, allowing the two myosin 'heads' and their motor domains to interact with actin and generate tension[3]. Most of the S2 rod appears to be a flexible coiled coil, but studies suggest that the structure at the N-terminal region is unstable[4–6], and unwinding or bending of the α-helices near the head–rod junction seems necessary for many of myosin's functional properties[7,8]. Here we show the physical basis of a

‡ Present address: Boston Biomedical Research Institute, 64 Grove Street, Watertown, Massachusetts 02472, USA.

© 2003 Nature Publishing Group